

Convex Optimization of Relative Orbit Maneuvers Using the Kustaanheimo-Stiefel Transformation

Jacob B. Willis
Robotics Institute
Carnegie Mellon University
5000 Forbes Ave.
Pittsburgh, PA 15213
jwillis@cmu.edu

Zachary Manchester
Robotics Institute
Carnegie Mellon University
5000 Forbes Ave.
Pittsburgh, PA 15213
zacm@cmu.edu

Abstract—As small-satellite constellations continue to grow in size and complexity, there is an increasing need for autonomous relative navigation and control capabilities. Many small satellites utilize non-impulsive low thrust propulsion or manipulation of perturbation forces such as differential drag for orbit control. These low-acceleration control technologies result in long time horizons over which the control actions must be planned and executed. Currently no dynamics model satisfies the computation, accuracy, and generalizability required for autonomous long-time-horizon control. This paper presents a relative-dynamics model based on the Kustaanheimo-Stiefel transformation. We demonstrate that it achieves equivalent or better accuracy compared to existing relative-orbit models in the literature. In addition, our Kustaanheimo-Stiefel model requires a small number of timesteps per orbit and easily incorporates low-acceleration control inputs. These features make it easily adaptable to convex trajectory optimization methods, which we demonstrate by solving a low-thrust orbital rendezvous problem over a time horizon of 75 orbits with a maximum $20 \mu\text{m/s}^2$ thrust constraint.

TABLE OF CONTENTS

1. INTRODUCTION.....	1
2. RELATED WORK	2
3. BACKGROUND	2
4. TRANSFORMING FROM CARTESIAN TO KS SPACE	3
5. RELATIVE KS DYNAMICS	3
6. COMPARISON OF RELATIVE-ORBIT MODELS	4
7. RELATIVE ORBITAL MANEUVERS VIA CONVEX OPTIMIZATION	4
8. CONCLUSIONS.....	6
ACKNOWLEDGMENTS	6
REFERENCES	6
BIOGRAPHY	7

1. INTRODUCTION

Small-satellite constellations promise increased ground coverage, higher re-visit rates, and improved sensing resolution. However, a key enabling technology for these constellations is effective, autonomous, relative navigation and control. Because of the size, weight, and power constraints of small satellites, non-impulsive control methods using low-thrust propulsion systems [1] and manipulation of perturbation forces through techniques such as differential drag [2] and solar-sails [3] are gaining traction. A large number of models for the relative motion between spacecraft exist; however, these models aren't well-equipped for the constant low acceleration produced by non-impulsive control systems. In particular, the low accelerations result in long time horizons

over which the control action must be planned and executed. When formulated using Earth-centered inertial coordinates, the resulting trajectory optimization problems require tens to hundreds of thousands of timesteps—much too large to perform autonomously on an embedded flight computer. In contrast, orbital-element-based models are not generalizable as they must be developed to handle the specific control inputs and perturbations a spacecraft encounters.

Recently, the size of nonlinear trajectory optimization problems for long-horizon orbital maneuvers has been reduced by transforming the orbital dynamics using the Kustaanheimo-Stiefel (KS) transformation [4]. The KS transformation lifts the three inertial position coordinates of the spacecraft into a four-dimensional representation in which the unperturbed Keplerian dynamics become linear and time invariant (LTI). We refer to the four-dimensional KS-lifted position coordinates as the “KS space.”

We apply the KS transformation to relative orbital maneuvers between spacecraft in low-Earth orbit. We modify the KS-transformed dynamics to include perturbation forces due to non-spherical gravity and low-thrust control inputs. These modifications result in nonlinear dynamics; however, since only the perturbation terms are nonlinear, the KS dynamics are better approximated by linearization than other relative dynamics formulations. This “near linearity” allows for significantly longer step sizes during numerical integration. We solve the relative orbital maneuver problem by linearizing the perturbed KS dynamics with respect to a reference orbit in KS space.

Our contributions include:

- A novel optimization-based method for smoothly transforming Cartesian states into lifted KS states
- A KS formulation of relative orbital dynamics that includes J2 perturbations and low-thrust control inputs
- Accuracy comparisons between the KS-based relative dynamics and several existing state-of-the-art relative orbital dynamics models
- A convex-optimization formulation of the orbital rendezvous problem using our KS-based relative-orbit dynamics
- An example computation of an optimal rendezvous trajectory for a small spacecraft in low-Earth orbit with very low thrust capability

The paper proceeds as follows: We describe related work on relative-orbit models and previous applications of the KS transform to orbital maneuvers in section 2. In section 3 we provide a description of Cartesian and KS transformed orbit dynamics. Section 4 describes our method for transforming smooth trajectories from Cartesian to KS coordinates. In section 5 we derive a relative orbital dynamics model using the KS transform, and in section 6 we compare this model

with other relative-orbit models found in the literature by computing the trajectory prediction error versus a numerically integrated ground truth. In section 7 we incorporate the KS relative-orbit model into a convex trajectory optimization formulation, and solve a low-thrust orbital rendezvous problem. We conclude in section 8 by summarizing our results and suggesting future research directions.

2. RELATED WORK

There is an extensive literature on relative-orbit models. Sullivan, Grimberg, and D’Amico [5] provide a survey of these models and perform extensive comparisons between them. In section 6, we compare our KS relative-orbital model with the Clohessy-Wiltshire (CW) [6]; Yamanaka-Ankersen (YA) [7]; and Koenig, Guffanti, and D’Amico (KGD) [8] relative-orbit models. These models are developed by linearizing and integrating either the nonlinear Cartesian equations of motion or the Gauss Variational Equations for the orbital elements.

The CW relative-orbit model has been used extensively since the 1960s. It assumes a Keplerian circular reference orbit, is linear-time-invariant, and is parameterized by time. The CW model has been developed for both Cartesian and curvilinear relative coordinate frames [9]; in our comparisons we use the Cartesian coordinates.

The YA relative-orbit model extends the CW model to Keplerian eccentric orbits. It is parameterized by the true anomaly and uses a normalized Cartesian relative state representation. It is considered the state of the art Cartesian relative state representation for arbitrary Keplerian orbits [5]. In the circular case, the YA model reduces to the CW model.

The KGD model uses relative orbital elements and reflects the state of the art in state transition matrices for perturbed elliptical orbits. It provides a significant increase in accuracy over the CW and YA models and has similar or better accuracy to other models in the literature [10], [5].

The Kustaanheimo-Stiefel transformation was originally introduced as a method for regularizing the numerical integration of perturbed two-body motion [11]. It extends the planar Levi-Civita transformation [12] to three dimensions, and provides exact linear-time-invariant equations of motion for unperturbed Keplerian orbits in three dimensions. To our knowledge, the first work applying the KS transform to the relative motion between spacecraft is by Eldin, who studied the KS transform in the context of unconstrained planar rendezvous maneuvers [13]. Thorne and Hall [14] use the planar KS transform to develop analytic expressions for minimum-time continuous-thrust orbit transfers. Hernandez and Akella [15] use the Levi-Civita transformation to find a Lyapunov control policy for finite-thrust orbital rendezvous from arbitrary orbital positions, illustrating the power of working in the Levi-Civita or (more generally) the KS coordinates. Perturbation forces were not considered in these previous works.

Recently, Tracy and Manchester [4] used the KS dynamics and nonlinear trajectory optimization to perform low-thrust transfers from a geostationary transfer orbit (GTO) to a geostationary orbit (GEO). The difference between the approach we present here and the approach in [4] is that we linearize the relative KS dynamics in the presence of perturbations, and perform convex optimization to compute rendezvous maneuvers between multiple spacecraft. Liu and Lu [16]

approach the satellite-rendezvous problem using successive convexification methods to approximate the nonlinear relative dynamics and to satisfy safety constraints. In contrast, the linear KS dynamics allow us to solve a single convex optimization problem.

3. BACKGROUND

Cartesian Orbit Dynamics

In inertial Cartesian coordinates, the unperturbed Keplerian dynamics of a satellite orbiting a massive body are

$$\ddot{x} = -\frac{\mu}{r^3}x, \quad (1)$$

where $x \in \mathbb{R}^3$ is the position vector relative to an inertial frame centered on the massive body, $r = \|x\|_2$, and μ is the standard gravitational parameter of the massive body. In low-Earth orbit, the perturbation of these dynamics is dominated by atmospheric drag and the non-spherical shape of the Earth. We capture the dominant non-spherical gravitational effects by including the J_2 acceleration [17],

$$a_{J_2} = -\frac{3}{2} \frac{J_2 \mu R_E^2}{r^5} \begin{bmatrix} \left(1 - 5 \left(\frac{x_3}{r}\right)^2\right) x_1 \\ \left(1 - 5 \left(\frac{x_3}{r}\right)^2\right) x_2 \\ \left(3 - 5 \left(\frac{x_3}{r}\right)^2\right) x_3 \end{bmatrix}, \quad (2)$$

where J_2 is the normalized J_2 spherical-harmonic coefficient for the Earth’s gravitational field, R_E is the radius of the Earth, and x_1, x_2, x_3 are the components of x along the axes of the Earth-centered inertial (ECI) coordinate frame. The J_2 perturbed Cartesian dynamics are then

$$\ddot{x} = -\frac{\mu}{r^3}x + a_{J_2}. \quad (3)$$

In this work, we focus on the effects of eccentricity and the J_2 perturbation, so we neglect atmospheric drag. However, the model we present can be readily extended to include drag forces.

The Kustaanheimo-Stiefel Transform

We now consider the transformation of eq. (3) into the four-dimensional KS space [18]. The transformation is not unique when transforming from Cartesian (\mathbb{R}^3) to KS space (\mathbb{R}^4), so we first define the transform from KS space to Cartesian.

Let $y \in \mathbb{R}^4$ be the KS variable corresponding to the Cartesian position $x \in \mathbb{R}^3$, and define the matrix

$$L(y) = \begin{bmatrix} y_1 & -y_2 & -y_3 & y_4 \\ y_2 & y_1 & -y_4 & -y_3 \\ y_3 & y_4 & y_1 & y_2 \\ y_4 & -y_3 & y_2 & -y_1 \end{bmatrix}. \quad (4)$$

The KS transformation from y to x is then

$$\begin{bmatrix} x \\ 0 \end{bmatrix} = L(y)y. \quad (5)$$

The fourth row of $L(y)y$ is always zero. The matrix $L(y)$ has some useful properties. In particular,

$$L^T(y)L(y) = L(y)L^T(y) = (y^T y)I \quad (6)$$

where I is the identity matrix. It follows that

$$\begin{aligned} r^2 &= x^T x = (L(y)y)^T L(y)y \\ &= y^T L^T(y) L(y) y = (y^T y)^2. \end{aligned} \quad (7)$$

The KS transformation also introduces a scaled fictitious time s that relates to real time by the inverse of the radius,

$$dt = rds. \quad (8)$$

We denote variables differentiated with respect to real time with a dot, $\dot{x} = dx/dt$, and variables differentiated with respect to the fictitious time with a prime, $y' = dy/ds$.

The KS transformed velocity is

$$\dot{x} = \frac{1}{r} x' = \frac{2}{y^T y} L(y) y'. \quad (9)$$

Under the KS transformation, the Keplerian two-body dynamics in eq. (1) become

$$y'' = -\frac{h}{2} y, \quad (10)$$

where

$$h = \frac{\mu}{r} - \frac{\dot{x}^T \dot{x}}{2} = \frac{\mu - 2y'^T y'}{y^T y} \quad (11)$$

is the total energy of the orbit. Because h is constant for unperturbed orbits, eq. (10) is a four-dimensional simple-harmonic oscillator. In the KS space, the dynamics of any Keplerian orbit are linear and time invariant.

Arbitrary Cartesian disturbance accelerations $d(x, \dot{x}) \in \mathbb{R}^3$ and control accelerations $u \in \mathbb{R}^3$, can be transformed to the KS dynamics. Under perturbation, eq. (10) becomes

$$y'' = -\frac{h}{2} y + \frac{y^T y}{2} L^T(y) \begin{bmatrix} u + d \\ 0 \end{bmatrix}. \quad (12)$$

With acceleration inputs, the energy h is no longer constant:

$$h' = -2y'^T L^T(y) \begin{bmatrix} u + d \\ 0 \end{bmatrix}. \quad (13)$$

To account for the energy dynamics, we define an augmented state:

$$z = \begin{bmatrix} y \\ y' \\ h \end{bmatrix} \in \mathbb{R}^9, \quad (14)$$

and write the perturbed dynamics

$$z' = f(z, u). \quad (15)$$

The disturbances $d(x, \dot{x})$ can be written as a function of y and y' as follows:

$$d(x, \dot{x}) = d(L(y)y, \frac{2}{y^T y} L(y)y') \triangleq d(y, y'). \quad (16)$$

For the remainder of this paper, we let d be the J_2 acceleration in eq. (3).

4. TRANSFORMING FROM CARTESIAN TO KS SPACE

For each Cartesian position, $x \in \mathbb{R}^3$, there is a one-dimensional submanifold of \mathbb{R}^4 such that any point y on that manifold satisfies the KS transform in eq. (5). For this reason, the inverse of eq. (5), transforming from Cartesian to KS space, is not unique. A single solution y can be found by algebraically inverting eq. (5) and arbitrarily choosing the value of one of the elements of y [18], [4]. Unfortunately, while the transformation between the Cartesian and KS spaces is smooth, this method exhibits singularities in the KS space and the transformation of a smooth trajectory into the KS space will not necessarily be smooth. Additionally, when computing the relative position between two KS states, this non-uniqueness leads to two degrees of freedom in the relative position and there may be a relative KS position with smaller norm.

To ensure that transformed trajectories are smooth, and to compute a relative position of minimum norm, we formulate the inverse KS transform as an optimization problem,

$$\begin{aligned} &\underset{y}{\text{minimize}} \quad (y - \bar{y})^T (y - \bar{y}) \\ &\text{subject to} \quad \begin{bmatrix} x \\ 0 \end{bmatrix} = L(y)y, \end{aligned} \quad (17)$$

where x is the Cartesian position we wish to convert and \bar{y} is the KS position we desire y to be close to. The solution, y^* , of this optimization problem is the KS position closest to \bar{y} that satisfies the KS transform. To convert points along a trajectory, we let \bar{y} be the transform of the previous point. If there is no logical \bar{y} , we let $\bar{y} = [1, 0, 0, 0]^T$. We solve (17) efficiently using Newton's method.

Figure 1 shows the difference between our proposed nearest state method and the common method. The lines shown are the trajectory of an orbit with unit amplitude and period. The trajectory was originally computed in Cartesian space and has been transformed to the KS space using the common method of fixing an arbitrary element of the state vector and our nearest-state method. The plot shows the transformed KS coordinates of the trajectory. In this case, the common method arbitrarily assigns $y_4 = 0$ to invert eq. (5). This results in the discontinuity at $t = 0.5$. Our nearest-state method, which minimizes the difference between each point and the previous one, produces a smooth trajectory.

5. RELATIVE KS DYNAMICS

To define the relative KS dynamics, we let z and u be the state and control of the deputy satellite, and we define the chief state \bar{z} and control \bar{u} . The relative state is $\delta z = z - \bar{z}$, the relative control is $\delta u = u - \bar{u}$, and the relative dynamics are:

$$\begin{aligned} \delta z' &= z' - \bar{z}' = f(z, u) - f(\bar{z}, \bar{u}) \\ &= f(\bar{z} + \delta z, \bar{u} + \delta u) - f(\bar{z}, \bar{u}) \\ &= \frac{\partial f}{\partial z}(\bar{z}, \bar{u})\delta z + \frac{\partial f}{\partial u}(\bar{z}, \bar{u})\delta u + \mathcal{O}(\|\delta z\|^2). \end{aligned} \quad (18)$$

Since the Keplerian dynamics for y'' are already linear, the higher-order terms in eq. (18) are due to the control inputs, perturbations, and the difference in energy between the deputy and chief orbits. The effect of these are orders

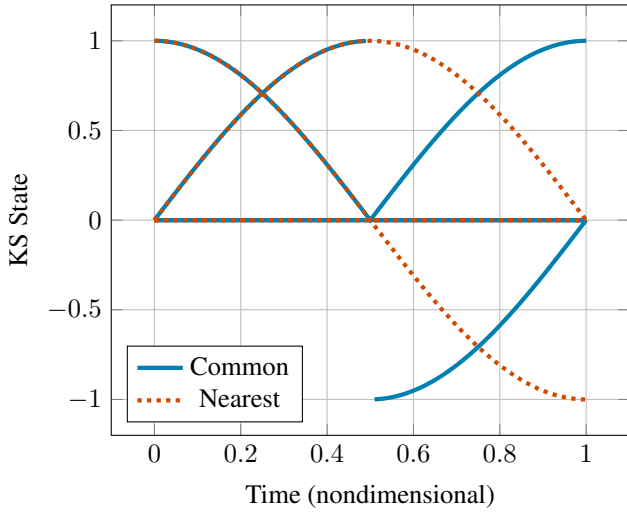


Figure 1. Cartesian to KS transformation of a unit orbit, comparing the non-smooth common method and our nearest state method.

of magnitude smaller than the Keplerian dynamics, so it is a very good approximation to drop the higher-order terms. This yields the linear-time-varying relative dynamics

$$\delta z' = \frac{\partial f}{\partial z}(\bar{z}, \bar{u})\delta z + \frac{\partial f}{\partial u}(\bar{z}, \bar{u})\delta u. \quad (19)$$

To find the discrete-time linear-time-varying relative dynamics, we numerically integrate the controlled state-transition matrix dynamics,

$$\Phi' = \begin{bmatrix} \frac{\partial f}{\partial z}(\bar{z}, \bar{u}) & \frac{\partial f}{\partial u}(\bar{z}, \bar{u}) \\ \mathbf{0}_{3 \times 9} & \mathbf{0}_{3 \times 3} \end{bmatrix} \Phi, \quad (20)$$

along a given trajectory \bar{z}, \bar{u} . We then define the discrete-time linear-time-varying state-space system

$$\delta z_{k+1} = A_k \delta z_k + B_k \delta u_k \quad (21)$$

where $A_k \in \mathbb{R}^{9 \times 9}$ contains the first nine rows and columns of $\Phi(s_{k+1}, s_k)$ and $B_k \in \mathbb{R}^{9 \times 3}$ contains the first 9 rows and last 3 columns of $\Phi(s_{k+1}, s_k)$. Since Φ is computed with the Jacobian of the J2-perturbed KS dynamics, the LTV dynamics include both periodic and secular effects of the J2 perturbation.

6. COMPARISON OF RELATIVE-ORBIT MODELS

We now compare our linearized KS relative-orbit state transition matrix (eq. (20)) with the CW, YA, and KGD linear relative-orbit state transition matrices. Table 1 summarizes the differences between these models. The procedure of section 5 is not unique to the KS dynamics, so we also use it to linearize the nonlinear Cartesian dynamics by substituting eq. (3) for f and x for z . We refer to the resulting model as the ‘‘LIN’’ model. In [8], the KGD model is developed for three different relative orbital element (ROE) states, the singular ROEs, quasi-nonsingular ROEs, and the nonsingular ROEs; the nonsingular ROEs are the most general of the representations, so we use them for our comparisons.

Figure 2 shows the root-mean-square (RMS) position error measured along trajectories propagated for one orbital period. The ground-truth orbits are a numerical integration of the J2-perturbed nonlinear equations of motion in eq. (3) using a high-accuracy adaptive Runge-Kutta method[19], [20]. The deputy initial conditions are perturbed with a range of offsets in mean anomaly, inclination, eccentricity, and semi-major axis while the other orbital parameters are held constant. We use the same reference orbit as in scenario 1 of Sullivan, et al. [5] for comparison with the relative-orbit models they present. Table 2 shows the reference orbit initial conditions used for the mean anomaly, inclination, and semi-major axis variation experiments.

As in [5], to compare performance on eccentric reference orbits, both the reference and deputy orbits are initialized with the same variation of eccentricity. All other initial orbital elements for the reference orbit match Table 2. The deputy orbit is offset from the reference orbit by 0.001 degrees in both mean anomaly and inclination. This corresponds to a distance of approximately 125 meters.

Figure 2 shows that our KS model exhibits significantly less propagation error than any of the other relative-orbit models. Since the reference orbit is circular for the mean anomaly, inclination, and semi-major axis plots, the CW, YA, and LIN models perform identically. On the eccentricity plot, the CW model exhibits higher error than the YA model, which again matches the LIN model. On the mean anomaly and inclination models, the KGD model exhibits higher error than the KS model within the small angles shown on the plot. The astute reader will notice that extrapolating the KS and KGD mean anomaly and inclination plots, the KS error does grow faster than the KGD error. While not shown, the difference between the KS and KGD error at large mean anomaly and inclination separation angles remains within an order of magnitude of each other. This should not detract from the excellent small-angle performance of the KS model, since relative-orbit models are most commonly used at deviations of less than 10 degrees in mean anomaly or inclination. For the semi-major axis variations, the KGD model exhibits higher error than any of the other models. As an additional note, the extensive use of orbital elements in the YA and KGD models leads to numerous degeneracies and singularities, significantly complicating their practical use. In contrast, the Cartesian and KS dynamics are globally smooth and well behaved.

7. RELATIVE ORBITAL MANEUVERS VIA CONVEX OPTIMIZATION

The LTV relative dynamics given by eq. (20) allow us to construct a convex trajectory optimization formulation of the orbital rendezvous problem. With the discretized dynamics in eq. (21), trajectories of length N can be computed by solving a convex optimization problem over $\delta z_{1:N}$, and $\delta u_{1:N-1}$:

$$\begin{aligned} & \underset{\delta z_{1:N}, \delta u_{1:N-1}}{\text{minimize}} && J(\delta z_{1:N}, \delta u_{1:N-1}) \\ & \text{subject to} && \delta z_{k+1} = A_k \delta z_k + B_k \delta u_k, \\ & && \delta u_k \in \mathcal{U}_k, \\ & && \delta z_k \in \mathcal{Z}_k, \end{aligned} \quad (22)$$

where $J(\delta z_{1:N}, \delta u_{1:N-1})$ is a convex cost function, and \mathcal{Z}_k and \mathcal{U}_k are convex sets.

The time steps in eq. (22) are scaled fictitious KS times.

Table 1. Comparison of Relative-Orbit Models

	Linear	Independent Variable	Reference Orbit	J2	State Representation
Clohessy-Wiltshire (CW)	✓	Real time	Circular	✗	Cartesian
Yamanaka-Ankersen (YA)	✓	True anomaly	Elliptical	✗	Normalized Cartesian
Numerically Linearized Cartesian (LIN)	✓	Real time	Elliptical	✓	Cartesian
Koenig, Guffanti, and D'Amico (KGD)	✓	Real time	Elliptical	✓	Orbital Elements
Kustaanheimo-Stiefel (KS)	✓	Fictitious time	Elliptical	✓	Augmented Quaternion

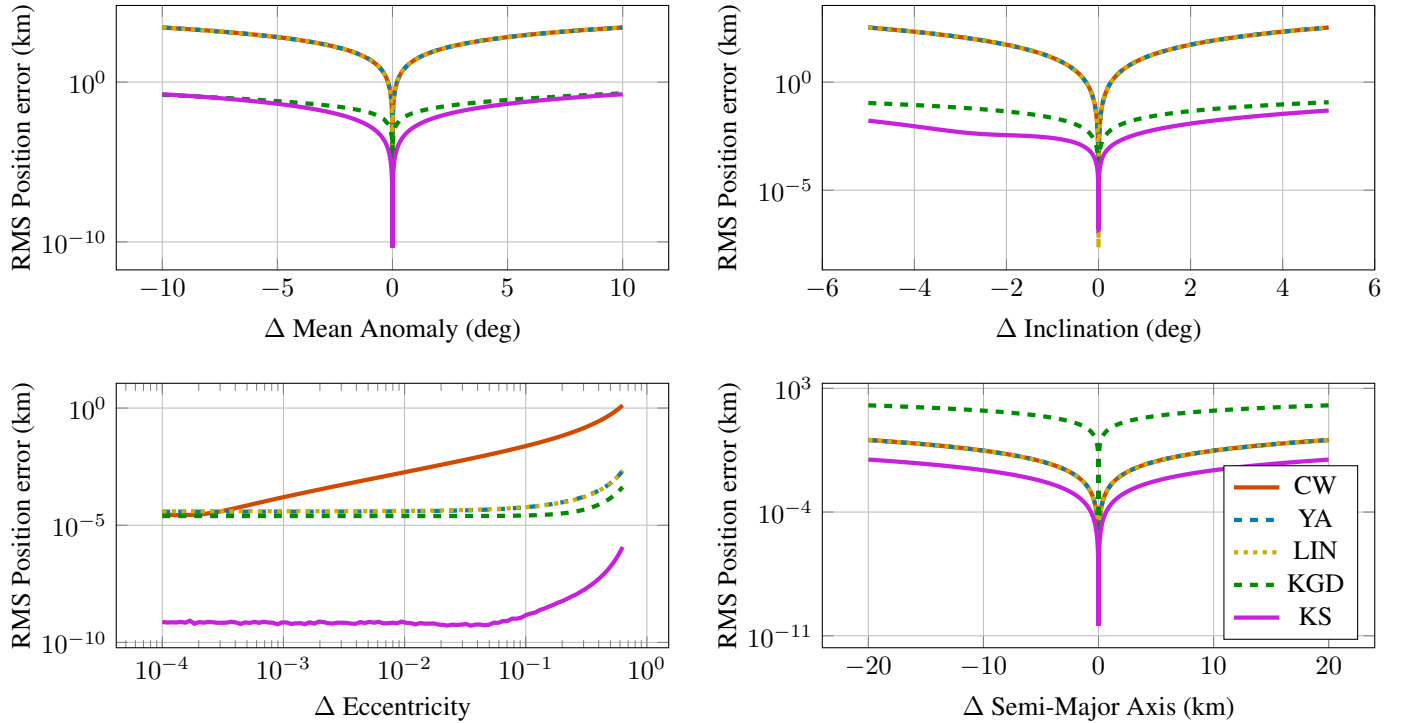


Figure 2. RMS position error along a single orbit with a range of initial variations in mean anomaly, inclination, eccentricity, and semi-major axis while the other orbital parameters are held constant. Lines correspond to the Clohessy-Wiltshire (CW), Yamanaka-Ankersen (YA), J2-perturbed linear-time-varying Kustaanheimo-Stiefel (KS) and the Koenig, Guffanti, and D'Amico (KGD) linear relative-orbit models. The ground truth is a numerical integration of eq. (3).

Table 2. Reference Orbit Initial Conditions for RMS Trajectory Error Plots in Figure 2

a	e	i	Ω	ω	M
750 + 6378 km	0.0	98.2°	0°	0°	0°

Once the optimal trajectory is found, the real times at which $\delta u_{1:N-1}^*$ should be applied are found by integrating eq. (8) along the chaser states,

$$t_k = \sum_{i=1}^k \|\bar{z}_k + \delta z_k^*\|^2 ds. \quad (23)$$

Low-Thrust Rendezvous Maneuver

We demonstrate the convex trajectory optimization with KS dynamics by solving a low-thrust rendezvous maneuver. The

orbits and relative states for this scenario are similar to the International Space Station final approach performed by Soyuz and SpaceX Dragon spacecraft. The target and chaser initial orbital elements, as well as the initial RTN state of the chaser with respect to the target, are given in Table 3. To formulate this problem in the context of eq. (22), we assume the target spacecraft is not producing thrust, but is experiencing perturbations, and integrate the target states with eq. (15) to compute A_k and B_k . We additionally right-multiply B_k by a rotation matrix which maps vectors in the target spacecraft RTN frame to Earth-centered inertial vectors. This allows us to compute the controls in the target RTN frame, which is a typical choice for formation flying problems [21]. The quadratic cost is,

$$J(\delta z_{1:N}, \delta u_{1:N-1}) = \delta z_N^T Q_N \delta z_N + \sum_{k=1}^{N-1} \delta z_k^T Q_k \delta z_k + \delta u_k^T R_k \delta u_k, \quad (24)$$

where $Q_* \succ 0$, $R_* \succ 0$. To demonstrate the long optimization horizon possible with KS dynamics, we use a maximum thrust acceleration constraint of $20\mu\text{m/s}^2$. This maximum thrust falls in the range of low-thrust, high specific impulse propulsion systems currently available for small satellites [1]. The optimization uses 20 timesteps per orbit and a 100 orbit horizon, resulting in 2000 knot points. A solution is computed once per orbit, and the controls from that solution are applied to the J2-perturbed nonlinear dynamics over the following orbit in a receding-horizon fashion. We solve these trajectory optimization problems using the convex quadratic program solver OSQP [22]. It takes approximately 6 seconds to integrate the discrete dynamics, set up, and solve this trajectory optimization on a MacBook Pro with an Apple M1 Pro processor.

The results of this maneuver are shown in fig. 3. The top-left plot shows that the position and velocity errors do not converge monotonically, but do converge to zero over time. The top-right plot shows the thrust control inputs over time. The thrust constraints are active for much of the first 50 orbits. The bottom two plots show the chaser trajectories on the radial-tangential plane and radial-normal plane.

8. CONCLUSIONS

We have shown that a relative-orbit-dynamics model based on the Kustaanheimo-Stiefel transformation that includes linearized J2 perturbations and control inputs is highly accurate and achieves higher accuracy than other state-of-the-art models in the literature. The KS relative dynamics model provides a linear-time-varying dynamics formulation that can be incorporated into standard estimation and control tools. Because the KS relative dynamics are very accurate, long-horizon prediction and trajectory-planning problems can be solved.

Our rendezvous demonstration provides one application of the KS relative dynamics. Many other scenarios are possible, including complex maneuvers with differential drag and solar sails. Additionally, safety constraints are an essential consideration in rendezvous or proximity operations problems that we will investigate in future work.

The code used to produce the results in this paper is available at <https://github.com/RoboticExplorationLab/KSRelativeOrbits>.

ACKNOWLEDGMENTS

This work was supported by the Department of Defense National Defense Science and Engineering Graduate Fellowship (NDSEG).

REFERENCES

- [1] K. Lemmer, “Propulsion for cubesats,” *Acta Astronautica*, vol. 134, pp. 231–243, 2017.
- [2] C. Foster, J. Mason, V. Vittaldev, L. Leung, V. Beukelaers, L. Stepan, and R. Zimmerman, “Constellation phasing with differential drag on Planet Labs satellites,” *Journal of Spacecraft and Rockets*, vol. 55, no. 2, pp. 473–483, 2018.
- [3] B. Fu, E. Sperber, and F. Eke, “Solar sail technology—A state of the art review,” *Progress in Aerospace Sciences*, vol. 86, pp. 1–19, 2016.
- [4] K. Tracy and Z. Manchester, “Low-thrust trajectory optimization using the Kustaanheimo-Stiefel transformation,” in *AAS/AIAA Astrodynamics Specialist Conference*, 2021, pp. 1–12.
- [5] J. Sullivan, S. Grimberg, and S. D’Amico, “Comprehensive survey and assessment of spacecraft relative motion dynamics models,” *Journal of Guidance, Control, and Dynamics*, vol. 40, no. 8, pp. 1837–1859, 2017.
- [6] W. Clohessy and R. Wiltshire, “Terminal guidance system for satellite rendezvous,” *Journal of the Aerospace Sciences*, vol. 27, no. 9, pp. 653–658, 1960.
- [7] K. Yamanaka and F. Ankersen, “New state transition matrix for relative motion on an arbitrary elliptical orbit,” *Journal of guidance, control, and dynamics*, vol. 25, no. 1, pp. 60–66, 2002.
- [8] A. W. Koenig, T. Guffanti, and S. D’Amico, “New state transition matrices for spacecraft relative motion in perturbed orbits,” *Journal of Guidance, Control, and Dynamics*, vol. 40, no. 7, pp. 1749–1768, 2017.
- [9] F. deBruijn, E. Gill, and J. How, “Comparative analysis of Cartesian and curvilinear Clohessy-Wiltshire equations,” *Journal of Aerospace Engineering*, vol. 3, no. 2, p. 1, 2011.
- [10] D.-W. Gim and K. T. Alfriend, “State transition matrix of relative motion for the perturbed noncircular reference orbit,” *Journal of Guidance, Control, and Dynamics*, vol. 26, no. 6, pp. 956–971, 2003.
- [11] P. Kustaanheimo, A. Schinzel, H. Davenport, and E. Stiefel, “Perturbation theory of Kepler motion based on spinor regularization.” 1965.
- [12] T. Levi-Civita, “Sur la résolution qualitative du problème restreint,” *Acta Mathematica*, vol. 30, p. 305, 1906.
- [13] H. N. Eldin, “Trajectory control in rendezvous problems using the regularization techniques,” *IFAC Proceedings Volumes*, vol. 3, no. 1, pp. 101–115, 1970.
- [14] J. D. Thorne and C. D. Hall, “Minimum-time continuous-thrust orbit transfers using the Kustaanheimo-Stiefel transformation,” *Journal of guidance, control, and dynamics*, vol. 20, no. 4, pp. 836–838, 1997.
- [15] S. Hernandez and M. R. Akella, “Lyapunov-based guidance for orbit transfers and rendezvous in Levi-Civita coordinates,” *Journal of Guidance, Control, and Dynamics*, vol. 37, no. 4, pp. 1170–1181, 2014.
- [16] X. Liu and P. Lu, “Robust trajectory optimization for highly constrained rendezvous and proximity operations,” in *AIAA Guidance, Navigation, and Control (GNC) Conference*, 2013, p. 4720.
- [17] F. L. Markley and J. L. Crassidis, *Fundamentals of spacecraft attitude determination and control*. Springer, 2014, vol. 1286.
- [18] E. L. Stiefel and G. Scheifele, *Linear and regular celestial mechanics: Perturbed two-body motion, numerical methods, canonical theory*. Springer, 1971, vol. 174.
- [19] C. Tsitouras, “Runge–kutta pairs of order 5 (4) satisfying only the first column simplifying assumption,” *Computers & Mathematics with Applications*, vol. 62, no. 2, p. 770–775, 2011.
- [20] C. Rackauckas and Q. Nie, “DifferentialEquations.jl—a

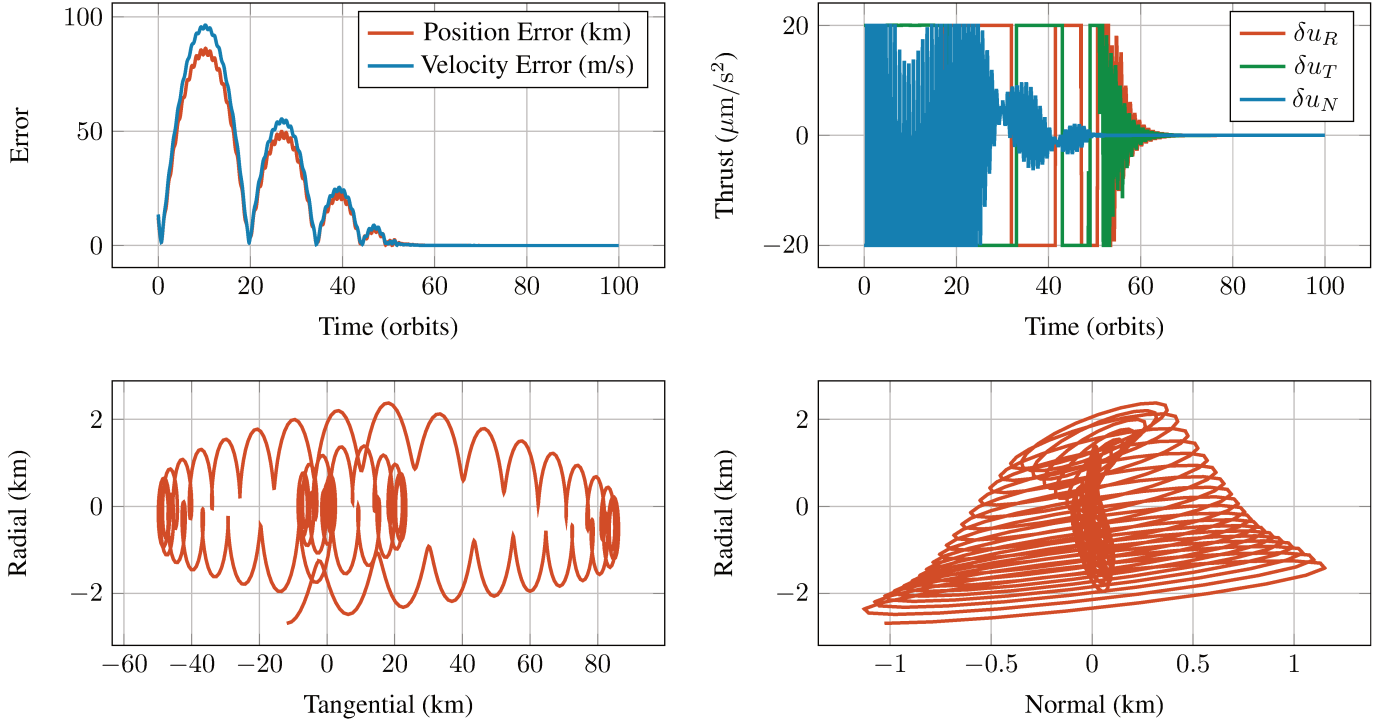


Figure 3. Position and velocity error, thrust control inputs, and radial-tangential-normal (RTN) trajectories for a low-thrust rendezvous maneuver.

Table 3. Initial Conditions for Low-Thrust Rendezvous in Figure 3

Orbital Elements	a	e	i	Ω	ω	M
Target	417 + 6378 km	0.0003	51.64°	0°	300°	0°
Chaser	415 + 6378 km	0.0004	51.65°	0°	300°	-0.1°
RTN State	x_R	x_T	x_N	\dot{x}_R	\dot{x}_T	\dot{x}_N
	-2.7 km	-11.9 km	-1.0 km	0.0033 m/s	4.9 m/s	0.67 m/s

performant and feature-rich ecosystem for solving differential equations in julia,” *Journal of Open Research Software*, vol. 5, no. 1, p. 15, 2017.

- [21] K. T. Alfriend, S. R. Vadali, P. Gurfil, J. P. How, and L. Breger, *Spacecraft formation flying: Dynamics, control and navigation*. Elsevier, 2009, vol. 2.
- [22] B. Stellato, G. Banjac, P. Goulart, A. Bemporad, and S. Boyd, “OSQP: An operator splitting solver for quadratic programs,” *Mathematical Programming Computation*, vol. 12, no. 4, pp. 637–672, 2020. [Online]. Available: <https://doi.org/10.1007/s12532-020-00179-2>

BIOGRAPHY



Jacob Willis is a PhD student in the Robotics Institute at Carnegie Mellon University. He received a BS and MS in Electrical and Computer Engineering from Brigham Young University in 2019 and 2021. His research interests include applications of numerical optimal control for autonomous aerospace systems, with recent work on small satellites and winged eVTOL micro-aerial vehicles.



Zachary Manchester is an assistant professor in the Robotics Institute at Carnegie Mellon University and founder of the Robotic Exploration Lab. He received a PhD in aerospace engineering in 2015 and a BS in applied physics in 2009, both from Cornell University. His research interests include control and optimization with application to aerospace and robotic systems with challenging nonlinear dynamics.